

## XANES characterization of $\text{UO}_2/\text{Mo}(\text{Pd})$ thin films as models for $\epsilon$ -particles in spent nuclear fuel

This content has been downloaded from IOPscience. Please scroll down to see the full text.

2013 J. Phys.: Conf. Ser. 430 012113

(<http://iopscience.iop.org/1742-6596/430/1/012113>)

View [the table of contents for this issue](#), or go to the [journal homepage](#) for more

### Download details:

IP Address: 131.169.95.180

This content was downloaded on 17/11/2016 at 08:46

Please note that [terms and conditions apply](#).

You may also be interested in:

[Actinide and lanthanide speciation with high-energy resolution X-ray techniques](#)

T Vitova, M A Denecke, J Göttlicher et al.

[Characterization of U\(VI\)-phases in corroded cement products by micro\(\)-spectroscopic methods](#)

J Rothe, B Brendebach, C Bube et al.

[High resolution X-ray emission spectroscopy: An advanced tool for actinide research](#)

T Vitova, B Brendebach, K Dardenne et al.

[Development of Fast Scanning Microscopic XAFS Measurement System](#)

T Tsuji, T Uruga, K Nitta et al.

[In situ two-dimensional micro-imaging XAFS with CCD detector](#)

H Tanida, H Yamashige, Y Orikasa et al.

[Structural transformation in Co-doped ZnS Nanoparticles](#)

Kai Chen, Qingteng Hou, Xueguang Dong et al.

[Colloidally prepared platinum nanoparticles deposited on iron oxide studied by XAFS](#)

E Piskorska-Hommel, D Arndt, T Wilkens et al.

## XANES characterization of $\text{UO}_2/\text{Mo(Pd)}$ thin films as models for $\epsilon$ -particles in spent nuclear fuel

M A Denecke<sup>1</sup>, T Petersmann<sup>2</sup>, R Marsac<sup>1</sup>, K Dardenne<sup>1</sup>, T Vitova<sup>1</sup>, T Prüßmann<sup>1</sup>, M Borchert<sup>3</sup>, U Bösenberg<sup>3</sup>, G Falkenberg<sup>3</sup> and G Wellenreuther<sup>3</sup>

<sup>1</sup>Karlsruhe Institute of Technology, Institut für Nukleare Entsorgung, Postfach 3640, D-76021 Karlsruhe, Germany

<sup>2</sup>European Joint Research Center, Institute for Transuranium Elements (ITU), D-76344 Eggenstein-Leopoldshafen, Germany

<sup>3</sup>Deutsches Elektronen-Synchrotron (DESY), Notkestr. 85, D-22607 Hamburg, Germany

E-mail: melissa.denecke@kit.edu

**Abstract.** X-ray absorption near edge structure (XANES) is recorded for nano- and micro-particles formed in Mo doped  $\text{UO}_2$  thin films (TFs) prepared by in situ sputter co-deposition and 1000°C tempering. These  $\text{UO}_2/\text{Mo}$  TFs are intended to serve as synthetic models for  $\epsilon$ -particles in spent nuclear fuel. We find that when Si is used as substrate, nano-sized zero-valent Mo particles form as desired. However, these are embedded in  $\text{USi}_3$ , which forms at the high temper temperatures. Micron-sized Mo-particles are formed when  $\text{SiO}_2$  is used as substrate. Using focussed X-ray beams of varying size (500 $\mu\text{m}$ , 25 $\mu\text{m}$  and 5 $\mu\text{m}$ ), these particles are characterized to be predominantly hexavalent Mo oxides, potentially with tetrahedral coordinated  $[\text{Mo(VI)O}_4]^{2-}$  at the surface and a  $\text{MoO}_3$ -like phase in the bulk. These TFs are poor synthetic models for spent fuel  $\epsilon$ -particles but do offer the opportunity to study changes in surface structures in response to stress/charge as a function of particle size.

### 1. Introduction

Spent nuclear fuel (SNF) consists of 95%  $\text{UO}_2$  and 5% mixture of radionuclides (RNs) and fission products, heterogeneously distributed throughout the fuel matrix in different phases, e.g., gases (Xe, Kr, I), oxides (including transuranic elements Pu, Np, etc.) and metallic precipitates or so-called  $\epsilon$ -particles (Pd, Mo, Rh, Ru, etc.) [1,2]. Systematic investigations of SNF matrix corrosion as an important source term for the mobilization of RNs are essential for evaluating SNF disposal safety [3,4]. We prepare  $\text{UO}_2/\text{Mo}$  thin films (TFs) for potential use as models to study the influence of  $\epsilon$ -particles on the surface corrosion of SNF. The TFs provide a less complex system and lower radiation fields than actual SNF samples, which allow systematic mechanistic investigations even in non-radioactive laboratories.

We determine how well these TF models mimic the SNF surface by thoroughly characterizing their composition, structure and morphology using numerous methods. Studies of  $\text{UO}_2/\text{Mo}$  TFs having varying Mo content prepared via *in situ* sputter co-deposition on different substrates (Si,  $\text{SiO}_2$  or  $\text{LaAlO}_3$ ) by means of 2-dimensional (2D) and 3-dimensional synchrotron-based imaging methods (scanning nano-/micro-XRF, scanning nano-XRD and XRF, holographic and ptychographic tomography) reveal that nano- and micro-sized Mo-particles form in TFs prepared on Si and  $\text{SiO}_2$

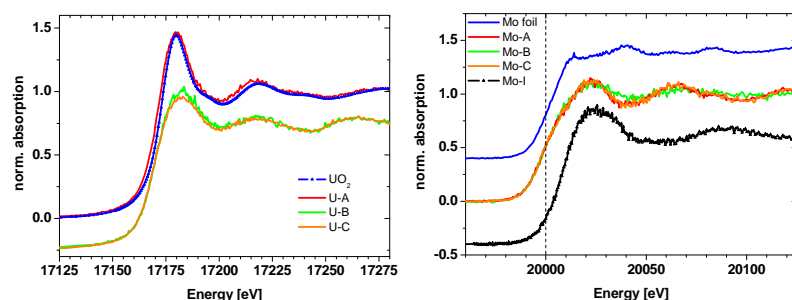


**Figure 1:** (left) U L3 XANES of  $\text{UO}_2$  and sample H measured at different positions. (right) Mo K- XANES of a  $\text{Mo}^0$ -foil (edge energy indicated as vertical dashed line), recorded at different positions of sample H and of a Mo hot spot in sample I (Mo-I). Designations A,B,C refer to the sample H phase at the position where the spectrum was measured: A=  $\text{UO}_2$ , B=  $\text{USi}_3$ , C= mixed phase region.

## 2. Experimental

Mo L3 edge spectra are recorded at the INE-Beamline for actinide research [6] at the ANKA synchrotron in fluorescence mode, using the low energy setup available there and a Si(111) double crystal monochromator (DCM) calibrated against the first inflection point in the Mo L3-XANES of a  $\text{Mo}^0$ -foil (2.52 keV). Both scanning XRF measurements and XANES measurements using a focused X-ray beam are performed at the hard X-ray Micro/Nanoprobe beamline P06 at PETRA III [7] and at HASYLAB beamline-L experimental station (DORIS at DESY). The X-ray beam is focused at P06 using a Kirkpatrick-Baez (KB) system equipped with Rh-coated silica mirrors, which in our experiment delivered an enlarged focal spot size of approximately  $2\mu\text{m}$  (H)  $\times$   $7\mu\text{m}$  (V) due to monochromator instabilities. At beamline-L a polycapillary half-lens is used to focus the beam to  $35\mu\text{m}$  (H)  $\times$   $22\mu\text{m}$  (V) at 23 keV. At both beamlines a Si(111) DCM is used and the beam energy calibrated against the first inflection point in the Mo K-XANES of a  $\text{Mo}^0$ -foil reference, defined as 20.0 keV.

Two  $\text{UO}_2$  TFs doped with 8 and 20 wt% Mo and around 500 nm thick are prepared via co-deposition of U and Mo onto  $\text{SiO}_2$  and Si substrates and tempering, designated as sample I and H, respectively (sample preparation is described in [5]). Samples are mounted at a  $45^\circ$  angle to the incident beam on a positioning stage for scanning in the y and z directions (2D) and positioning the x-axis into the beam focus. A Vortex-90EX silicon drift detector (SII Nanotechnology USA) is used at the INE-Beamline and beamline-L and a Vortex-EM at P06 for collecting X-ray fluorescence radiation. Mo K (U L3) edge XANES are recorded from Mo (U)-rich areas identified in distribution maps reconstructed from the scanning  $\mu$ -XRF data.

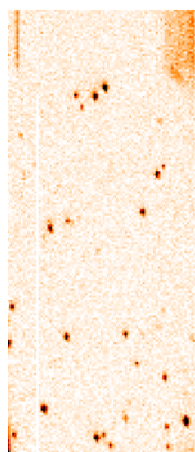


**Figure 2:** Mo distribution in a  $5000 \times 2100 \mu\text{m}^2$  area of sample I, 25  $\mu\text{m}$  step size and 0.5 s counting time.

## 3. Results and discussion

In previous  $\mu$ XRF/ $\mu$ -XRD studies performed at the ESRF ID22Ni using a 100 nm focussed beam, we found that for TFs prepared on Si substrates and tempered at  $1000^\circ\text{C}$  (sample H) the  $\text{UO}_2$  partially reacts with the substrate, thereby forming  $\text{USi}_3$  with Mo localized as 100-400 nm nanoparticles in  $\text{USi}_3$  grain boundaries [5]. Uranium L3 XANES recorded at beamline-L using a  $\sim 25\mu\text{m}$  focussed-beam at different sample areas identified to be composed of  $\text{UO}_2$ ,  $\text{USi}_3$  and a mixture of these two phases are depicted in Figure 1 (left). The XANES from the  $\text{UO}_2$  area (U-A) is similar to a bulk  $\text{UO}_2$  reference spectrum but with a broadened white line at  $\sim 17180$  eV, as well as indication of a lengthening of the average U-O distance, evident as a shift of the first EXAFS resonance at  $\sim 17216$  eV to lower energy (due to the relation  $\Delta E \propto 1/R(\text{U-O})^2$  [8]). The U L3 XANES spectra measured at the sample area comprised the mixed  $\text{UO}_2/\text{USi}_3$  phases (U-C) are more similar to

substrates and tempered at  $1000^\circ\text{C}$  ( $600^\circ\text{C}$  was not sufficient); when  $\text{LaAlO}_3$  is used as substrate and tempered at  $1000^\circ\text{C}$ , Mo does not aggregate but is found concentrated at the substrate surface [5]. In this report we characterize the Mo-particles observed to form in these TFs using X-ray absorption near-edge structure (XANES) at the Mo K-edge and the L3-edges of both Mo and U.

the XANES recorded in an area composed solely of  $\text{USi}_3$  (U-B) suggesting that U is mostly present as  $\text{USi}_3$  in the mixed phase.

All Mo K XANES recorded at various areas randomly distributed across sample H lie within 1.2 eV to one another and although their edge energies are near that for  $\text{Mo}(0)$ , their XANES fingerprint does not resemble  $\text{Mo}^0$ -foil at all. The Mo K-XANES recorded at exactly the same sample positions as the U L3 spectra are shown in Figure 1 (right). The edge energies are near that for  $\text{Mo}(0)$  and well below energies expected for  $\text{Mo(IV)}$  and  $\text{Mo(VI)}$  (around 20003.5 and 20007.5 eV [9]). In contrast to the U L3 results above, Mo K XANES recorded in the mixed phase area of sample H (Mo-C) is essentially identical to that from the  $\text{UO}_2$  area (Mo-A) and less similar to the  $\text{USi}_3$  sample area XANES (Mo-B). The bulk Mo L3 edge data measured at the INE-Beamline at ANKA for sample H at different positions on the sample is shown in Figure 3 (lower curves, top). The L3 edge spectra line up with that for the  $\text{Mo}(0)$  L3 XANES and lie below the  $\text{Mo(IV)O}_2$  and  $\text{Mo(VI)O}_3$  reference spectra, indicating that the mean valence of Mo nanoparticles observed to form in the tempered  $\text{UO}_2/\text{Mo}$  TFs on Si is zero. Similar to the K edge data, the sample H XANES fingerprint does not resemble that for  $\text{Mo}^0$ -foil; the white lines are at least twice as intense and the resonance above the white line visible in the  $\text{Mo}(0)$  spectrum is absent. Presumably these differences result from the small size of the particles (narrowing of final state 4d band and loss of extended coordination structure).

In Mo distributions reconstructed from scans of small areas of sample I using a nano-sized beam at ESRF ID22-NI, no Mo hot spots were found. In large area XRF scans of sample I (Figure 2) measured at beamline-L with a  $\mu$ -sized beam, 25-150  $\mu\text{m}$  sized Mo hot spots are revealed, which are distributed randomly and widely spaced in the  $\text{UO}_2$  TF. A Mo K-XANES recorded from one of the larger hot spots is shown in Figure 1 (right, bottom curve). The spectrum show a single broad main absorption and its edge energy lies approximately at 20007.3 eV, which is close to the value expected for  $\text{Mo(VI)}$  [9]. Bulk Mo L3 edge data (Figure 3, top) for sample I recorded at two different positions on the sample show well-resolved features, as the life time broadening due to the L3 core hole is considerably reduced. The white line is split into  $t_{2g}$  and  $e_g$  states for the (distorted)  $\text{O}_h$  symmetry of the reference oxides; the  $t_{2g}$  being partially occupied in  $\text{Mo(IV)}$  ( $d^2$ ). The sample I spectra qualitatively more resemble the  $\text{Mo(VI)}$  L3 signal with a strong  $t_{2g}$  intensity. The L3 XANES energy position is evaluated from the value of the arctan step function obtained in XANES fits, compared to the reference spectra. The result of this analysis is shown in Figure 3 (bottom). The relationship between reference oxidation state and edge energy was not strictly linear so we modelled the calibration curve with a polynomial function. Using this curve, the Mo oxidation state in sample I determined for the two L3 XANES spectra is 3.8 (I1) and 5.2 (I2). For comparison, fits to the spectra as linear combination of the  $\text{MoO}_2$  and  $\text{MoO}_3$  reference spectra gave slightly different mean Mo valence values in I1 and I2, 4.7 and 5.4, respectively. The quality of least square fit results, however, indicates that these two reference compounds are not sufficient to model sample I L3 spectra. This is likely due to the presence of tetrahedral coordinated  $\text{Mo(VI)}$  in this sample (see below).

In order to explore the reason for measuring different mean Mo oxidation states in one and the same sample I, we use a  $\sim 5 \mu\text{m}$  beam at the P06 microprobe experimental station to measure Mo K XANES of individual Mo particles  $< 5 \mu\text{m}$  in size and compared these to those recorded at different positions of

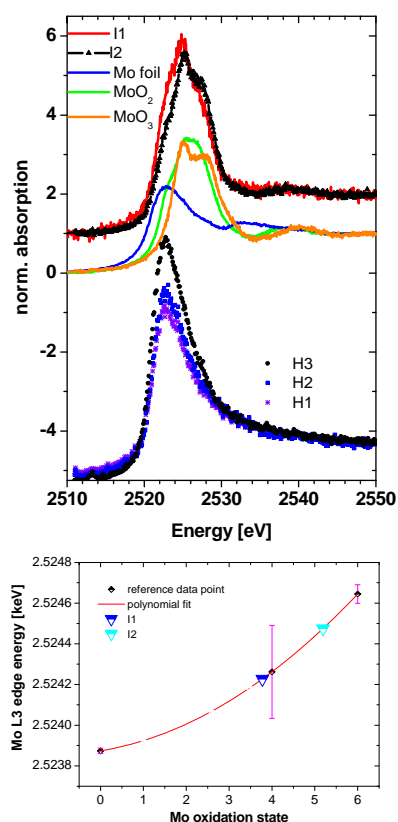


**Figure 3:** (top) Mo L<sub>3</sub>- XANES recorded at different positions on sample H (lower curves) and for sample I (upper curves), compared to  $\text{Mo}(0)$ ,  $\text{Mo(IV)}$ , and  $\text{Mo(VI)}$  reference spectra (middle curves). (bottom) Calibration curve of L<sub>3</sub>-edge energies versus Mo oxidation states. See text for details.

a particle at least 10 times larger. The results are shown in Figure 4. Particles studied having dimensions of the beam size or smaller exhibit a strong pre-peak at around 20005 eV, which is a signature for tetrahedral coordinated  $[\text{Mo(VI)O}_4]^{2-}$  (cf. the XANES for  $\text{CaMoO}_4$ ). This feature is absent or reduced to a shoulder (similar to  $\text{MoO}_3$ ) on the rising absorption edge in most pixels studied (spectra 1-3), but clearly (and reproducibly) visible in the XANES measured on the outer rim of the particle (#4). The Mo K energy position at half the edge jump of the XANES without a pre-peak all lie about 8 eV above the Mo(0) XANES, indicative of hexavalent molybdenum. We find no evidence for Mo(IV). Summarizing results for this particular particle: we observe a mixture of a  $\text{MoO}_3$ -like phase and also tetrahedral coordinated  $[\text{Mo(VI)O}_4]^{2-}$ , which is particularly evident at the pixel located at the particle rim. The average XANES from spectra 1 through 4 is shown in Figure 4 (#5), where the main absorption peak is broadened and the contribution of tetrahedral coordinated Mo(VI) reduced to a mere shoulder, which is imaginably a trend towards the sample I spectrum in Figure 1 measured with a  $\sim 25 \mu\text{m}$  beam. We interpret the two observations that 1) both the smallest particles and the rim of a large particle exhibit the largest tetrahedral coordinated Mo(VI) signal and that 2) the particles studied have Mo in its hexavalent state as suggesting charge compensation at the Mo-particles surface occurs through reduction of the number of O atoms coordinated to Mo (tetrahedral surface versus octahedral bulk coordination).

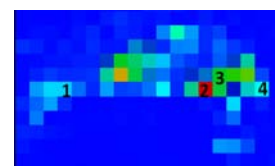
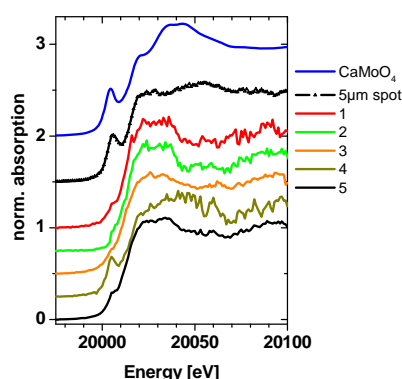


**Figure 4:** (left) Mo K-XANES measured in sample I for a  $5 \mu\text{m}$  pixel Mo hot spot and a  $\sim 60 \mu\text{m}$  wide Mo particle at the various positions (1-4) indicated in the Mo distribution map (above). Each pixel is  $5 \times 5 \mu\text{m}^2$ . XANES #5 is the average of spectra 1-4.

#### 4. Conclusions

These results show that none of the substrates or temper programs used produces satisfactory SNF  $\varepsilon$ -particle models. While nano- and micron-sized Mo particles are formed in the  $\text{UO}_2/\text{Mo}$  TF systems studied, these particles are either not embedded in the desired  $\text{UO}_2$  substrate or are present in oxide form, instead of the desired metallic state. The oxide particles, however, do offer the opportunity to study changes in surface structures in response to stress/charge as a function of particle size. It may be possible to prepare Mo(0)-particles embedded in  $\text{UO}_2$  on Si substrates through tempering at temperatures below  $1000^\circ\text{C}$ , but above  $600^\circ\text{C}$ .

#### Acknowledgments

We thank PETRAIII, HASYLAB and ANKA for the granted beamtime.

#### References

- [1] Kleykamp, H 1985 *J Nucl Materials* **131**(2-3) 221
- [2] Bruno J, Ewing R 2006 *Elements* **2** 34.
- [3] Johnson LH, et al. Spent Fuel. In Radioactive waste forms for the future, Lutze, W (Ed) 1988, pp 635-698
- [4] Shoesmith DW 2000 *J Nucl Materials* **282** 1
- [5] Denecke MA, et al. 2012 *MRS Spring Meeting Proceedings* **1444**, mrss12-1444-y01-05doi:10.1557/opl.2012.1159
- [6] Rothe J, et al. 2012 *Rev Sci Instrum* **83** 043105
- [7] Schroer CG, et al. 2010 *Nucl Instrum Methods* **A616** 93
- [8] Denecke MA *Proceedings of the OECD-NEA Workshop on Speciation, Techniques and Facilities for Radioactive Materials at Synchrotron Light Sources*, Grenoble, France, 4-6 October 1999, pp. 135-41.
- [9] Ressler T, Jentoft RE, Weinhold J, Günter MM, Timpe O 2000 *J Phys Chem* **B104**, 6360